AN ANALYSIS ON LOCAL HYDROGEN CONCENTRATION IN THE LARGE DRY PWR CONTAINMENT OF ULCHIN 3,4 IN KOREA

S.W. Hong, H.D. Kim*, and S.H. Chung**

ABSTRACT

The local hydrogen concentration was analyzed during two different severe accident scenarios (TMLB' and medium size LOCA) using CONTAIN code for the Ulchin 3,4 PWR containment type which is under construction in Korea. Sensitivity studies on the equivalent fraction of zirconium oxidation in the reactor vessel and the flow loss coefficient in the flow path between compartments were also carried out in order to investigate the effect of the these parameters on the local hydrogen concentration. Finally, the effect of temperature and turbulence intensity on the flame velocity was evaluated, and a sample calculation was performed by updating the model of the CONTAIN code. The calculated results show that the maximum local hydrogen concentration appears in the cavity compartment. The hydrogen burn, however, is not likely to occur in this compartment for both scenarios due to low oxygen concentrations. Hydrogen burns are more likely to occur at the steam generator compartments for TMLB' accident and at the reactor vessel annulus compartment during medium size LOCA. When the equivalent fraction of in-vessel zirconium oxidation is assumed to be 75 %, the possibility of detonation is much more increased. The change of flow loss coefficients between flow paths about 2 times affects on the magnitude of the maximum local hydrogen concentration but nearly no influence on the timing and the location of the compartment attaining the maximum local hydrogen concentration. The local hydrogen concentration in the compartments seems to be stratified after vessel failure but to be stabilized afterwards. When temperature and turbulence intensity are considered in the flame velocity model, the flame speed is much greater than the previous results, but the containment load is not increased very much.

* : Korea Atomic Energy Research Institute
** : Seoul National University

AN ANALYSIS ON LOCAL HYDROGEN CONCENTRATION IN THE LARGE DRY PWR CONTAINMENT OF ULCHIN 3,4 IN KOREA

S.W. Hong, and H.D. Kim
Korea Atomic Energy Research Institute

S.H. Chung
Seoul National University

1. INTRODUCTION

Since TMI-2 accident demonstrated that a large quantity of hydrogen could be generated during a severe accident, extensive research has been performed on the hydrogen combustion and control in light water reactor containment. In the NUREG-1150[1] report, it is pointed out that one of the important issues during the severe accident is the hydrogen combustion since it may cause the early containment failure together with direct containment heating.

For a large dry PWR containment, it is generally believed that hydrogen deflagration itself may not threaten the containment integrity. If hydrogen is locally concentrated, however, the deflagration to detonation transition(DDT) might occur and threaten the containment integrity. Thus, to maintain the containment integrity and mitigate the possibility of detonation during a severe accident, it is necessary to control the hydrogen combustion by reducing the local hydrogen concentration such as through deliberately burning the hydrogen with igniters.

In order to determine the number and location of igniters, analysis of local hydrogen concentration in the containment is essential. The local hydrogen concentration is affected by accident scenarios that determine the release location of source data, the flow model between compartments, and the equivalent fraction of in-vessel zirconium oxidation. The compartmentalization of containment is also important and has to be divided by considering the characteristics of containment geometric structure,

This paper focuses on the prediction of the local hydrogen concentration during two different severe accident scenarios of the TMLB' and the medium LOCA using CONTAIN code[2]. The reference plant are Ulchin 3,4 units, which are under construction in Korea and equipped with Westinghouse type of large dry PWR containment. The containment is divided by sixteen subcompartments by taking into account the containment geometric characteristics. The thermal hydraulic source data and the corium composition data for the TMLB' and medium LOCA scenarios were obtained from the results of MAAP 3B[3] calculation. The sensitivity studies were performed for the equivalent fraction of in-vessel zirconium oxidation and the effect of flow loss coefficient between flow paths.

The regulatory position in Korea for the hydrogen burn issue during a severe accident is not established yet, but planned to comply with the 10 CFR 50.34(f) for Ulchin 3,4 units. The 10 CFR 50.34(f) requires that 100 % metal water reaction of active core should be controlled, that the global hydrogen concentration should be maintained below 10 %, and that hydrogen control devices must be installed. It is expected that the results of this study could be used as base data to suggest the locations for of hydrogen igniters to be installed in order to prevent and mitigate hydrogen combustion when the postulated severe accidents occurred in Ulchin 3,4.

2. ANALYSIS OF LOCAL HYDROGEN CONCENTRATION

In numerous analyses for PWRs with large dry containment, hydrogen concentration has been calculated under the assumption of uniform hydrogen distribution in the containment. This assumption implies that the hydrogen in the containment is well mixed and only a global burning is considered. However, this can not be fully validated with the actual accident condition since containment is separated by many small compartments and hydrogen with steam would be released either from the reactor vessel or from the break position of the primary system to a specific location of a containment compartment.

Recent experimental and analytical studies show that the hydrogen mixing phenomena and local hydrogen concentration in the containment should be carefully investigated. According to the results of ISP-29[4], the HDR Hydrogen Distribution Experiment E11.2 post-test analysis, it is pointed out that the flow loss coefficient is important when lumped parameter code such as CONTAIN and MELCOR [5] code are used. The analyses of the NUPEC and HDR experiments using the CONATIN code [6] show also the limitations of the code for prediction of hydrogen stratification due to the lumped model. Nevertheless, CONTAIN code predicts the local hydrogen concentration reasonably except for the region of cells such as source compartment and dead-end compartment.

2.1 Input Model and Definition for Calculation Cases

The Ulchin 3,4 containment, which is Westinghouse type of large dry PWR containment, has a large containment volume of 2.73E6 ft^3. It is larger than that of typical PWR containment such as Zion(2.71E6 ft^3) and Surry(1.80E6 ft^3). In addition, the heat structure surface area is about 2 times bigger than that of Zion or Surry plant. One may expect that these large containment volume and heat structure surface area could decrease global hydrogen concentration and reduce the possibility of the hydrogen burn during a severe accident. The plant is also designed that the cavity is directly connected to the steam generator compartment so as to easily establish the natural convection flow inside the containment. The geometry and volume of cavity under the reactor vessel are another distinguished features of this containment. It has a large floor area to

satisfy the coolability conditions of the corium and a small capture volume to mitigate the direct containment heating which are recommended in the EPRI APWR URD.

Figure 1 shows the nodalization of the containment. It is nodalized into sixteen sub-compartments by taking into account containment geometric characteristics, including an external environment. The sum of each compartment volume and surface area of the structures corresponds to the data designated in the PSAR[7] of Ulchin 3,4 units. The detail information of the compartments such as compartment name, volume, number of heat structure, and compartment height between lower and upper for the each sub-containment, are described in Table 1.

Table 2 shows junction data between compartments. All the flow paths are normally open paths except the junctions of 2 and 24. The junction no. 2 connecting compartment 1 and 3 is normally closed by the cavity access door with size of 3'x7'. This door can be open to the outside of the cavity by pressure difference of 3 psi between each side of door. The junction no. 24 represents the flow path connected from the instrument tube exit to the refueling pool through cavity vertical column. This flow path can be formed to cavity outside by pressure difference of 9 psi between each side of door. Generally, the flow loss coefficient is a function of the concentration coefficient and a Reynolds number. However, it is difficult to determine the proper values for accident analysis since flow junctions have complicate paths and flow rates between junctions are not constant. , The values of the flow loss coefficient used in this paper remain in the range of between 0.5 for nearly opened flow path and 1.5 for complicate flow path.

Figure 2 shows the overflow water transport processes and Table 3 presents the overflow data for water stream. When steam is condensed on the compartment wall and water level inside the compartment is above the designated height, water overflows and transports to other compartments. Finally, all overflowed water is collected into the cavity(compartment no.1) and a sump located at the containment annulus(compartment no. 8, 11). From these overflow data, the cavity condition is determined to be either wet or dry when corium is released into the cavity after reactor vessel failure.

The amount of released materials from the primary system to various locations of containment such as steam, liquid water, hydrogen, molten core debris, and radioactive gases and aerosols, so-called source data, is taken from the calculation results of MAAP code for both scenarios.

Before the vessel failure, the materials from the primary system are released through the safety relief valves in case of TMLB', whereas for medium size LOCA accident, those are released through the broken part into the steam generator compartment. After the reactor vessel failure, the remaining source materials inside the primary system are puff-released into the reactor cavity for both scenarios. For both accident sequences, liquid, steam and hydrogen are released into the cavity during 58 s and 10 s after vessel failure, respectively. To model CORCON and VANESA module in CONTAIN code, molten corium is assumed to be released when the reactor vessel fails. The MCCI(Molten Core Concrete Interaction) in the cavity is assumed to start at the vessel failure for both scenarios.

Calculations were performed for six different cases(Table 4). Base case is to predict local hydrogen concentration for the TMLB' scenarios. Case 1 is carried out for evaluation of the effects on the local concentration when 75% of in-vessel zirconium oxidation was assumed since MAAP 3B code predicted rather low in-vessel zirconium oxidation about 33.8% compared with other code results. Case 2 is to assess containment loads in case of the auto ignition. Case 3 is for the case of medium LOCA scenarios that the primary system pressure is low. Case 4 and 5 are to examine effects of the flow loss coefficients on the local hydrogen concentration. In case 4, the same value of the flow loss coefficient 1.5 was applied for the whole flow path. In case 5, the flow loss coefficients of 0.5 for junction no. 20, 21, 22, 23, are used because these junctions are totally opened. Otherwise 1.5 is used for other junctions.

2.2 Results

In all cases, the magnitudes of the pressure with time in all of the compartments were nearly same. Maximum pressure for non-burning case appeared when the release of inventory in the reactor vessel finished. In case 2 where auto ignition was assumed, the first burn occurred in the steam generator compartment at 11,400 s, that is, 94 s elapsed after the vessel failure. After then, many burns occurred in reactor vessel annulus, cavity door area, steam generator compartment, and, containment annulus intermittently. The burns propagated four times in one compartment into other compartments when propagation condition was satisfied. The first propagation occurred from steam generator compartment(comp. no. 4) to containment annulus (comp. no. 8) and to pressurizer compartment(comp. no. 15) at 15,489 s, the second propagation from steam generator compartment(comp. no. 5) to containment annulus (comp. no. 11) and to polar crane compartment(comp. no. 14) at 15,724 s, the third propagation from steam generator compartment(comp. no. 4) to and to pressurizer compartment(comp. no. 15) at 19,746 s, and the last propagation from steam generator compartment(comp. no. 4) to steam generator compartment comp. no. 5) at 33,199 s. In case 2, maximum pressure appeared at the first burn propagation. In all cases, maximum pressure was not over the design pressure(54 psig) of Ulchin 3,4 containment even though the local hydrogen burns occurred. The accident scenario after the reactor vessel failure is described for the base case here.

Figure 3 describes the general flow direction/pattern at 14,006 s after the accident initiation. The gases flow according to the sequential order started from the cavity(comp. no 1) to the cavity door area(comp. no 3), steam generator B(comp. no 4), polar crane compartment B(comp. no 10), upper dome compartment B(comp. no 12), upper dome compartment A(comp. no 13), polar crane compartment A(comp. no 14), steam generator compartment A(comp. no 5), and steam generator compartment B. Similar flow pattern is maintained until end of the calculation time 40,000 s.

Figure 4 shows the accumulation energy consumed to boil the coolant in the cavity and the amount mass of steam generated by boiling. After vessel failure, steam is rapidly generated during

about 2,000 s because high corium sensible heat is transferred to the coolant. This rapid generation of steam results in the decrease the mole fraction of the hydrogen concentration in the cavity.

Figure 5 shows the amount of the zirconium consumed by the oxidation with steam and the hydrogen generated during the reaction after the unoxidized zirconium in the reactor vessel is released into the cavity. The zirconium was completely oxidized within 30 minutes. In base case, the highest hydrogen concentration appeared in the cavity compartment when the unoxidized zirconium within the reactor vessel was completely oxidized after released in the cavity(Figure 6). The maximum hydrogen concentration at steam generator compartment reached at the end of the hydrogen release from the reactor vessel because the amount of hydrogen released from the vessel is added to the amount of hydrogen generated by zirconium oxidation

Table 5 shows the time of the maximum hydrogen concentration for the cavity and steam generator compartments. The local hydrogen burn in the cavity(comp. no. 1) is not likely to occur because the oxygen concentration is nearly zero percent. With the same reason, the local hydrogen burns are not also likely to occur in the reactor vessel annulus(comp. no. 2) and cavity door area compartment(comp. no. 3) though the local hydrogen concentrations are higher than those of steam generator compartments. In the steam generator compartments(comp. no 4,5), however, although oxygen concentration is lower and steam concentration is higher than the generally accepted spontaneous burn criteria, the possibility of hydrogen burn and DDT can not be excluded because the hydrogen concentration is high as much as 11 % and would be increased if steam condenses or spray is operating. Figure 7 shows the hydrogen concentration distribution in the containment 1 minute after the vessel failure.

When the in-vessel zirconium oxidation fraction is assumed up to 75% (case 1), the hydrogen concentrations are higher than that of the base case. The local detonation is still not likely to occur due to low oxygen concentration in cavity door and reactor vessel annulus area. However, the possibility of hydrogen burn and DDT in steam generator compartments(comp. no. 4,5) increases because hydrogen concentration about 22% is much higher than the hydrogen concentration needed for detonation. For case 1, the maximum hydrogen concentration in the cavity reaches after reactor vessel failure since much of hydrogen which is not released and remains in the vessel was puff-released at that time (Figure 6). Therefore, the time to be reached to the highest hydrogen concentration in the cavity could be changed according to the zirconium oxidation fraction in the reactor vessel.

In case of the medium LOCA (case 2), unlike to base case, the high hydrogen concentration appears in the reactor vessel annulus compartment. This is because the cavity door connecting the cavity and steam generator compartment is not allowed to open during medium LOCA accident since the primary system pressure is low. Therefore, the flow path is mainly formed through the reactor vessel annulus. Figure 8 shows the hydrogen distribution in the containment at 80,000 s after the accident initiation. The hydrogen concentration in all compartments except for the cavity and dead-end volume(comp. no. 6 and 7) is nearly uniform. In the cavity compartment, various

gases during MCCI are generated. CONTAIN code is not seemed to describe properly the hydrogen distribution in the dead-end compartment as indicated from the previous studies.

Figure 9 shows the effect of the flow loss coefficient on the hydrogen concentration in the cavity. Although same values of the flow loss coefficients for the junction connected with the cavity are used(see the Table 2 and Table 4), the magnitude of the hydrogen concentration in the cavity is different. Figure 10 shows the distribution of hydrogen concentration with time in the steam generator compartment (comp. no 4). The change of the flow loss coefficient affects to the magnitude of the maximum local hydrogen concentration, but the difference of the maximum hydrogen concentration is rather small in this case. The location and the time for the maximum local hydrogen concentration in the containment are not changed. Therefore, a little change in the flow loss coefficient does not have much influence on the local hydrogen concentration in the steam generator compartment even though it affects the redistribution process of the hydrogen concentration and the decrease rate of mole fraction of hydrogen from the peak value to 0.04 is different for each case.

3. UPDATE OF THE FLAME VELOCITY

The treatment of combustible gases such as hydrogen and carbon monoxide in the CONTAIN code was adopted from the HECTR[8] code developed at SNL for hydrogen behavior analysis in the containment. In this model, flame speed is internally calculated based on the initial mole fraction only. However, it is known that when flames pass through obstacles, flames accelerate and the effective deflagration speed can be greatly increased. This is due to both the increase in flame front area by flame folding and the local increase of burning velocity by increase turbulence. Also, initial gas temperature and pressure have an effect on the burning velocity. Therefore, the flame speed has to be determined by the initial temperature and pressure, as well as initial mole fraction. The geometry of the compartment should also be considered because the presence of obstacles such as various components and structures in the containment is important factor to increase the flame velocity.

3.1 Model

The model for the flame speed in CONTIAN code was updated using turbulent-burning velocity suggested by Koroll, Kumar and Bowles[9]. They measured laminar and turbulent burning velocities of hydrogen-air mixture experimentally using the double-kernel technique for a range of hydrogen concentrations between 9% and 70% by volume and suggested simple correlation for the turbulent-burning velocity. This correlation can accommodate the flame speed depended on the initial mole fraction, initial temperature and pressure, and geometry of the compartment. The detail model for flame speed is as follows:

$$S_u(T) = S_{uo}\,(298)\,(\alpha/\alpha_o)^{1/2}\,[1 - \chi/\chi_L]\,(T/298)^n \qquad (1)$$

$$S_u(T,st) = S_u(T)\,(\alpha_{st}/\alpha_a)^{1/2}\,[1 - \chi_{st}/\chi_{Lst}] \quad (2)$$

$$S_t = S_u\,[1 + B\,(u'/S_u)^2]^{1/2} + u'' \quad (3)$$

From equation (1) and (2), it can be seen that laminar burning velocity increases as temperature increases and decreases as the steam concentration increases. In equation (3), the turbulent burning velocity is expressed as a function of the turbulence intensity, u', and flame generated turbulence, u", that can be approximated by the relationship as:

$$u'' = S_u[1 - \exp(-u'/S_u)]\,(\varepsilon - 1)/\sqrt{3} \quad (4)$$

From the above correlation, the following relationship between flame velocity and burning velocity can be obtained from the conservation of mass if the burnt gases are stationary and the pressure is constant.

$$V_f = S\,\rho_u / \rho_b \quad (5)$$

3.2 Results

To examine the effect of the new flame velocity, a sample calculation was carried out for large break LOCA scenarios. The containment was modeled as a single compartment. The composition of atmosphere conditions at the time when the burn has occurred consists of the hydrogen 12.39 %, oxygen 7.51 %, steam 55 % and nitrogen 24.8 %. The initial gas temperature is 391.8K and pressure is 2.47E5 Pa, respectively.

Figure 11 shows the turbulent velocity used in the CONTAIN code and in the updated model. The laminar flame velocity which is the function of temperature and pressure variations during the hydrogen burn, increases as the temperature increases. Also, it can be seen that steam can decrease the flame velocity. The turbulent flame velocity in updated model is much larger than those from the original CONTAIN code in the range 25 to 35 times. The turbulent flame velocity decreases with temperature since the density ratio of unburned to burnt gas decreases as temperature increases. Therefore, the temperature and turbulence effect can transfer the deflagration to the DDT because the flame velocity rapidly increases. The increase of the flame velocity is expected to reduce the burn time as is shown Figure 12. The burn time is about 50 s in the original CONTAIN code but it is about 2 s in the update model. This shortening of burn time increases the containment loads. The containment pressure in the original CONTAIN code and updated model is about 7.5E5 Pa and 8.5E5 Pa, respectively. In addition to the initial gas conditions, when turbulent effect is considered to the flame velocity, the possibility of DDT increases even though containment loads are not increase largely.

4. CONCLUSIONS AND DISCUSSIONS

The local hydrogen concentrations for containment types which are under construction in Korea, were predicted using the CONTAIN code. Local detonation might possibly occur at the steam generator compartments in TMLB' and in the reactor vessel annulus compartment during medium LOCA since the hydrogen and oxygen concentration in these compartments are rather higher compared with other compartments. When the equivalent fraction of zirconium oxidation in the reactor vessel is assumed to be 75 %, the possibility of detonation exists in many compartments. Therefore, if one want to maintain the hydrogen concentration below the value stated in the 10CFR 50.34(f) with the 100 % oxidation of zirconium, it is necessary to install hydrogen concentration control devices such as igniters. It would also decrease the possibility of DDT. The change of the flow loss coefficient about 2 times between the flow path has an effect on the magnitude of the maximum local hydrogen concentration, but no influence on time and location of compartments appearing the maximum local hydrogen concentration. The local hydrogen concentration in the compartments does not seem to be uniformed soon after the vessel failure but to be stratified afterwards. It is noted that the time for maximum local hydrogen concentration is within one minute after the reactor vessel failure for both scenarios. In the future, the sensitivity calculations for spray operation are to be continued.

The model for the flame speed in the CONTIAN code was updated to consider the effect of the initial mole fraction, initial temperature and pressure, and turbulence intensity using the suggested model of Koroll, Kumar and Bowles[9]. The flame velocity is set as constant in original CONTAIN code as 0.6 m/s but increases up to 25m/s in the updated model when the hydrogen mole fraction is 12.5%. Although, the containment loads in the updated model are not much increased than those of the original CONTAIN code, the possibility of DDT increases because flame velocity is considerably increased. This updated model for the flame velocity is to be investigated further by verifying with the experiment results.

REFERENCE

1. USNRC, "Severe Accident Risks : An Assessment for Five Nuclear Power Plants", NUREG-1150 (Vol. 1,2), June1989.
2. K.K. Murate, et al., "Users Manual for CONTAIN 1.1 : A Computer Code for Severe Nuclear Accident Containment Analysis", SNL, NUREG-CR5206, SAND87-2306, R4, Nov. 1989.
3. MAAP Version 3.0B Manual.
4. H. Karwat "Distribution of the Hydrogen within the HDR-Containment under Severe Accident Conditions, Final Comparison Report", OECD-CSNI-ISP-29, Aug. 1992
5. SNL, "MELCOR 1.8.2 Computer Code Manual", Feb. 1993.

6. ISP-35 Individual Presentation, "Notification of the Second Workshop on International Standard Program No. 35, NUPEC Hydrogen Distribution Test", NEA/SEN/SIN/WG4, Sep.1993.
7. Ulchin 3&4 PSAR, KEPCO
8. S.E. Dingman et al., "HECTR Version 1.5 User's Manual", SNL, NUREG/CR-4507,Apr. 1986.
9. G.W. Koroll, R.K Kumar, and E.M. Bowles, "Burning Velocities of Hydrogen-Air Mixtures", COMBUSTION and FLAME 94 : 330-340,1993.

NOMENCLATURE

B=16
i = Burned gas
j = Unburned gas
M = Mole
Po= Initial pressure
Q = Reaction heat
R = Gas constant
S = Burning velocity
S_t = Turbulent burning velocity
S_u = Laminar burning velocity
T= Gas temperature
Ti = Initial temperature
TMW=Total molecular weight of unburned gas
TMWB=Total molecular weight of burned gas
Tf= Gas temperature after burn
u' = Turbulence intensity
st= Steam
α= Thermal diffusivity of mixture
α_a= Thermal diffusivity of H2/air mixture
α_o= Thermal diffusivity of H2/oxygen
α_{st}= Thermal diffusivity of H2/air/steam mixture
χ_{st} = Steam mole fraction in the mixture
χ = Mole fraction of diluent gas in mixture
χ_H = Oxygen mole fraction
η = Mole ratio H2-oxygen
η_a = Mole ratio of H2-air
ε = Density ratio
ρ_u = Unburned gas density
ρ_b = Burned gas density.

CORRELATIONS

$n = A + C(0.42 - \chi_H)$

where,

A=1.571, C= 0.3839, for $[\chi_H] < 0.42$

= - 0.2476, for $[\chi_H] > 0.42$

$S_{uo} = 0.00166\eta^5 - 0.053\eta^4 + 0.674\eta^3 - 4.251\eta^2 + 11.84\eta - 0.604$

TMW =xs*mws + (1-xs-xh)*mwa + xh * mwh

TMWB = (xs + xh) * mws - (1-xs-xh)*mwa - 0.5 * xh * mwo

$$Tf = \frac{Q + (\sum MiCpi)Ti}{\sum MjCpj}$$

$\chi_{Lst} = 50.7 - 24.43\ \ln(\eta_a) - 18.5\ [\ln(\eta_a)]^2$, for $0.2 < \eta_a < 3$

$\chi_L = 83.1 + 6.14\ \ln(\eta) - 9.68\ [\ln(\eta)]^2$

$\varepsilon = \rho_u / \rho_b$

$\rho_u = Po\ TMW / (R\ Ti)$

$\rho_b = Po * TMWB / (R\ Tf)$.

Table 1. Nodalization of the Containment

Comapartment #	Compartment Name	Volume (m^3)	Number of Heat Structure	Compartment Height (ft)
1	Reactor cavity & instrument tunnel	475	8	55 - 112
2	Reactor vessel annlus	74	6	80.6 - 116
3	Cavity door area	111	4	86 - 114
4	S/G comp. B	3205	9	86 - 167
5	S/G comp. A	3313	9	86 - 167
6	RDT comp.	111	3	86 - 99
7	Regenerative Hx room	66	4	114 - 138
8	C/V annulus area A	5263	11	86 - 142
9	Refuling pool	1609	4	100.5 - 142
10	Polar crane comp. B	17332	8	142 - 230
11	C/V annulus area B	5168	11	86 - 142
12	Upper dome comp. B	11065	2	230 - 302
13	Upper dome comp. A	11065	2	230 - 302
14	Polar crane comp. A	17801	6	142 - 230
15	PZR comp.	305	3	122 - 185
16	Environment	1E+15	0	100

Table 2. Junction Data between Compartments

Junction	From	To	Flow Area (m^2)	AVL	CFC	Junction	From	To	Flow Area (m^2)	CFC
1	1	2	1.25	0.39	1.5	14	6	11	1.76	1.5
2	1	3	1.67	0.70	1.5	15	8	11	65.22	0.5
3	2	4	5.61	0.39	1.5	16	8	14	32.09	0.5
4	2	5	5.61	0.39	1.5	17	9	10	105.60	0.5
5	2	9	3.26	0.45	0.5	18	9	14	87.75	0.5
6	3	4	7.92	1.48	0.5	19	10	11	28.903	0.5
7	3	5	7.92	1.48	0.5	20	10	12	756.51	0.5
8	3	7	1.38	3.89	0.5	21	10	14	1177.51	0.5
9	4	5	14.14	1.32	1.0	22	12	13	756.51	0.5
10	4	10	152.70	16.3	0.5	23	13	14	756.51	0.5
11	4	11	3.80	0.15	1.5	24	1	9	3.9	1.0
12	5	8	5.07	0.18	1.5	25	11	15	1.95	1.0
13	5	14	149.00	16.3	0.5	26	15	10	28.50	0.5

Table 3. Flood Data of the Each Compartment

Comp. #	Floor Area(m^2)	Max Depth (m)	Overflood Comp. #	Elevation Drop (m)
1	64.8	10	1	
2	15	0.001	1	7.28
3	14	0.001	1	9.45
4	119	0.01	3	0.01
5	119	0.01	8	0.01
6	22	0.001	11	0.01
7	6	0.001	3	8.53
8	290	10	8	0.01
9	89	0.01	2	6.05
10	445	0.01	11	26.82
11	253	10	11	10.01
12	756	0.01	10	26.82
13	756	0.01	14	26.82
14	503	0.01	8	26.82
15	13	0.01	11	10.97

Table 4. Matrix of Calculation

Cases	Accident Scenarios	W or w/o Burn	Zr oxidation Fraction(%) in R.X	CFC
Base Case	TMLB'	w/o Burn	33.8	Same as Table 1
Case 1	TMLB'	w/o Burn	75.0	Same as Table 1
Case 2	TMLB'	Burn	33.8	Same as Table 1
Case 3	MLOCA	w/o Burn	27.8	Same as Table 1
Case 4	TMLB'	w/o Burn	33.8	1.5 for all junctions
Case 5	TMLB'	w/o Burn	33.8	0.5 for junction 20,21,22,23 1.5 for others

Table 5. Maximum Hydrogen Concentration and Gas Concentration in the Compartments

	Comp. #	Time(sec)	O_2	H_2O_V	H_2	CO	CO_2
Base Case	1	13,200	~ 0.0	75.3	21.5	2.7E-7	9.5E-6
	2	11,356	~ 0.0	87.5	12.2	1.3E-7	1.9E-6
	3	11,356	~ 0.0	87.5	12.2	2.3E-7	1.9E-6
	4	11,356	1.5	82.0	11.0	3.9E-7	1.3E-6
	5	11,356	2.0	79.7	10.8	3.2E-7	1.2E-6
Case 1	1	11,356	~ 0.0	75.8	24.2	1.4E-7	1.3E-6
	2	11,356	~ 0.0	76.0	24.0	1.4E-7	1.3E-6
	3	11,356	~ 0.0	75.8	24.1	1.4E-7	1.3E-6
	4	11,356	1.3	71.6	21.9	2.4E-7	1.0E-6
	5	11,356	1.7	70.7	21.5	2.4E-7	1.0E-6
Case 3	2	25,078	2.4	24.9	12.1	5.1	3.2E-5
	3	75,000	11.6	18.1	9.2	13.1	4.6
	4	79,078	11.3	18.8	9.1	13.2	5.2
	5	79,078	11.3	19.1	9.1	13.2	5.2

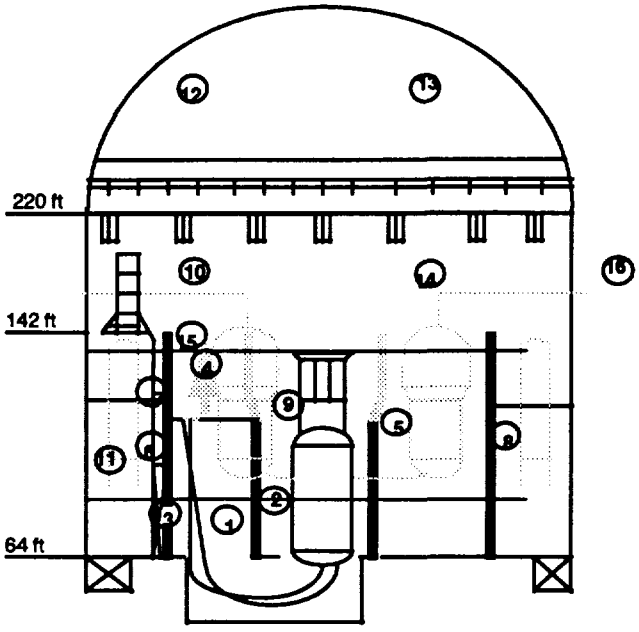

Fig. 1 Compartmentalization of the Containment

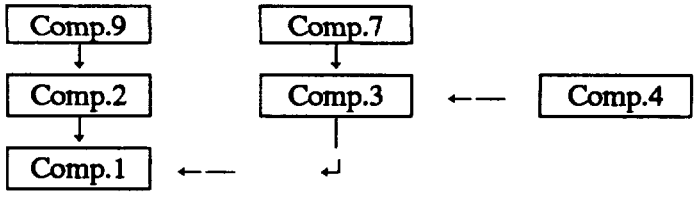

Fig 2-1 Overflow Path No. 1

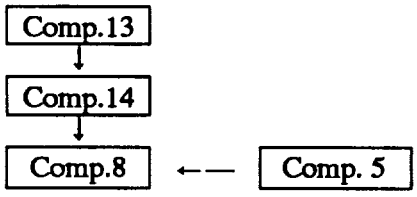

Fig 2-2 Overflow Path No. 2

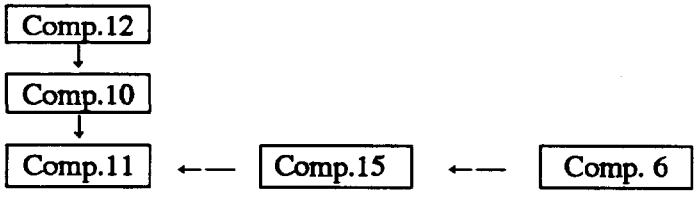

Fig 2-3 Overflow Path No. 3

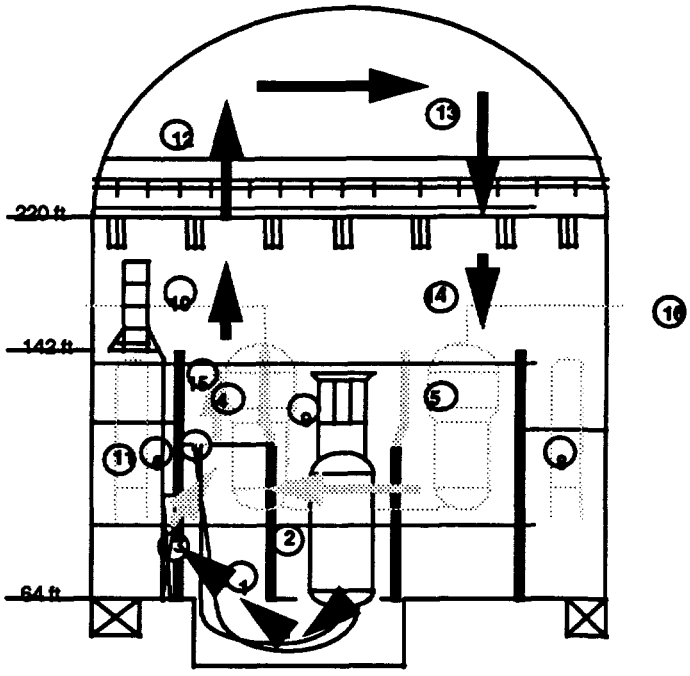

Fig. 3 Main Flow Pattern at 3,000 sec after Reactor Vesser Failure
(Accident Time : 14,000 sec)

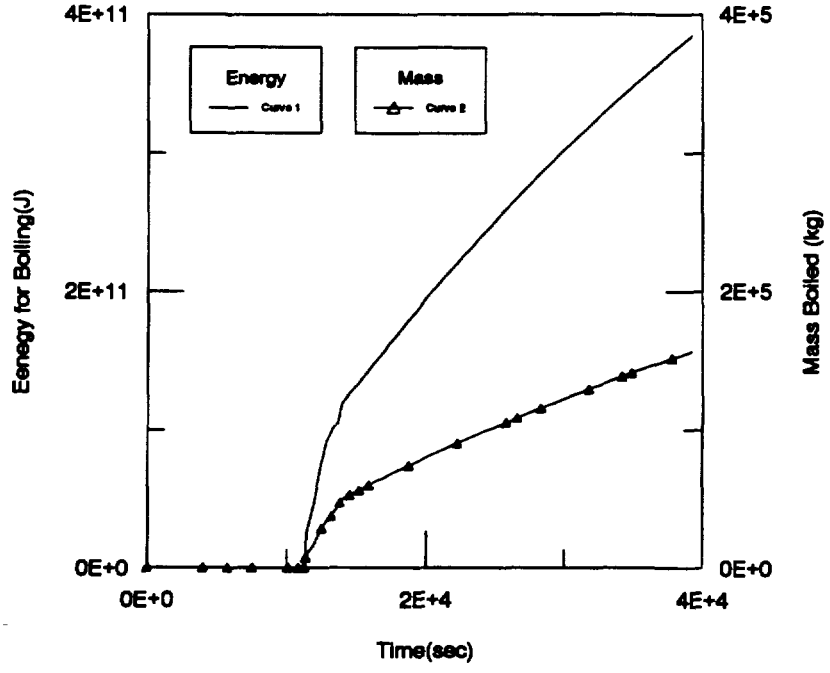

Fig. 4 Accumulation Energy and Steam Mass in the Cavity

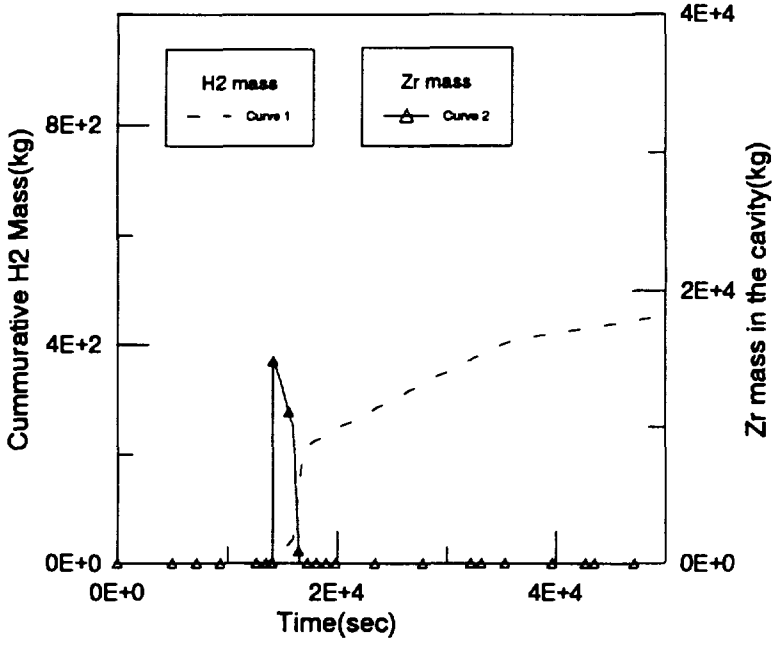

Fig. 5 Accumulative H2 Mass and Zr Mass in the Cavity

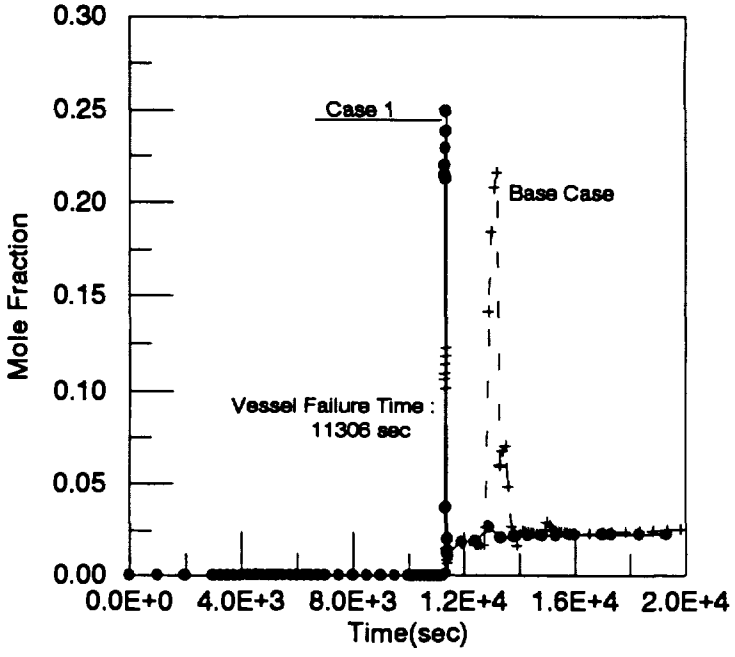

Fig. 6 Hydrogen Concentration in the Cavity for Base case and Case 1

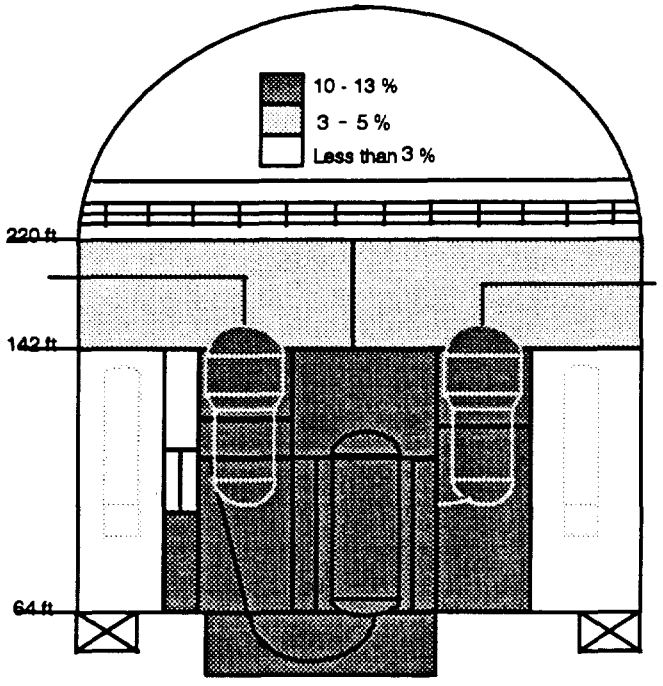

Fig. 7 Hydrogen Concentration Distribution at 11,356 sec for TMLB'

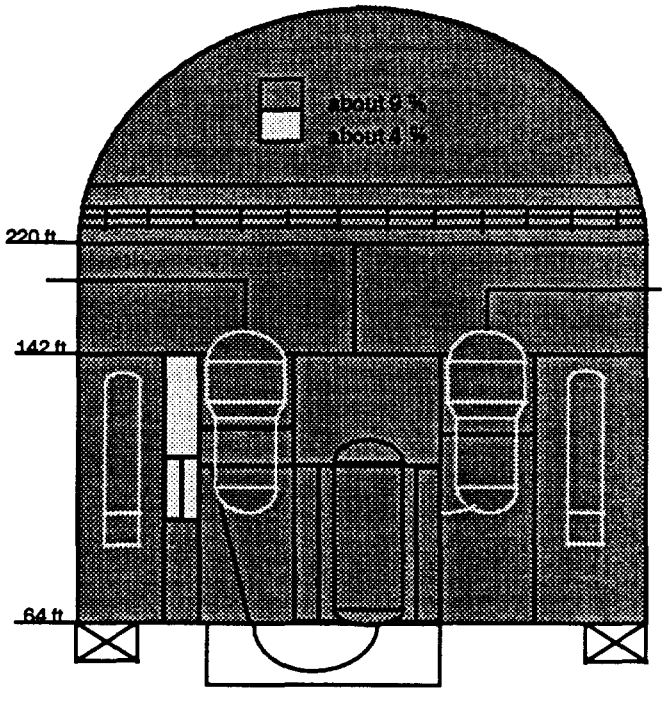

Fig. 8 Hydrogen Concentration Distribution at 80,000 sec for Medium LOCA

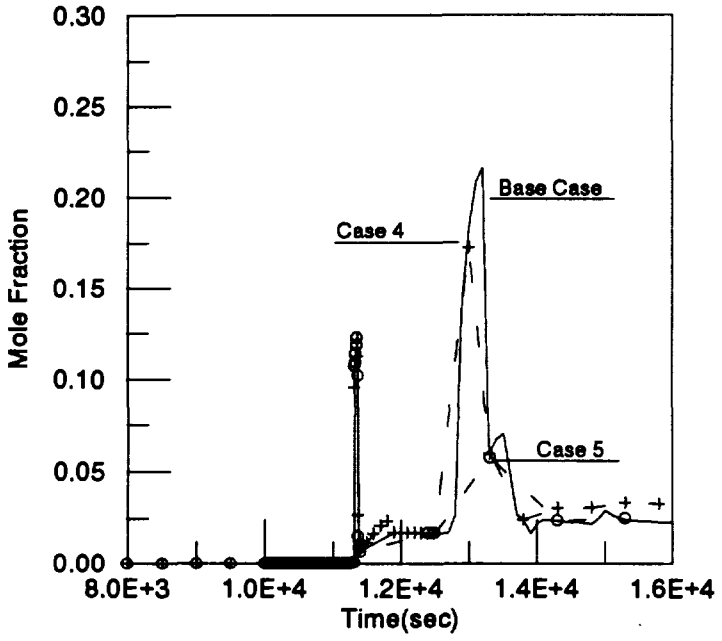

Fig. 9 Hydrogen Concentration in the Cavity for Base case, Case 4, and Case 5

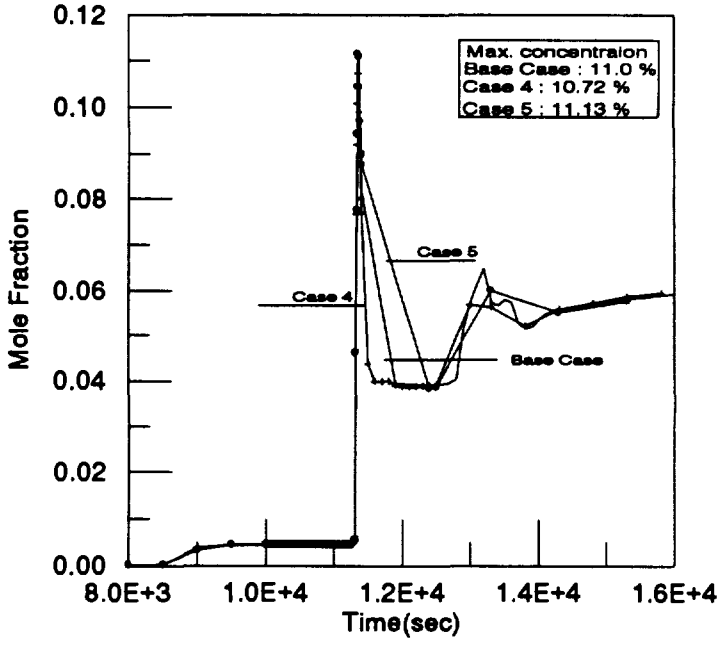

Fig. 10 Hydrogen Concentration in the S/G for Base case, Case 4, and Case 5

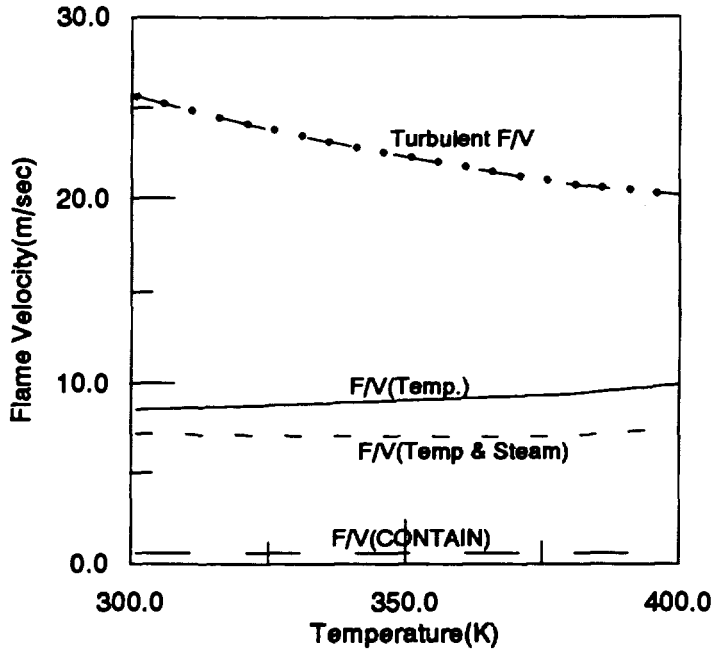

Fig. 11 Flame Velocity with Temperature

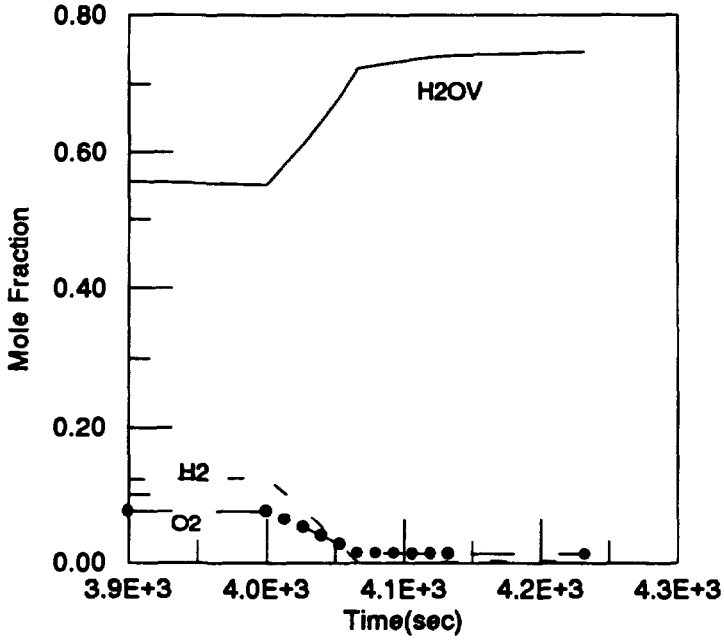

Fig. 12-1 Gas Concentration with Time in Old Model

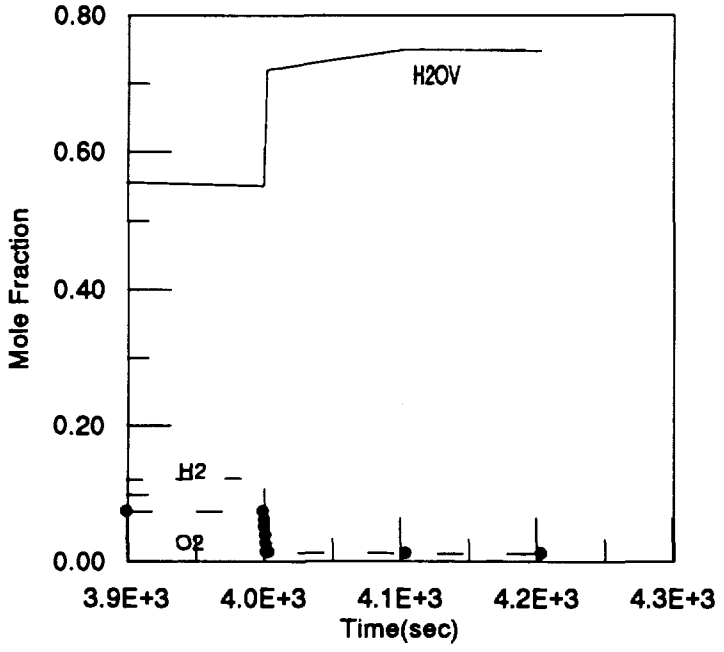

Fig. 12-2 Gas Concentration with Time in Updated Model